

## **Novel aerosol assisted plasma deposition of PEG containing coatings for non-fouling application.**

Annalisa Treglia<sup>a</sup>, Fabio Palumbo<sup>\*b</sup>, Roberto Gristina<sup>b</sup>, Cosima Damiana Calvano<sup>c</sup>, Tommaso Cataldi<sup>a</sup>, Francesco Fracassi<sup>a</sup>, Pietro Favia<sup>a,b</sup>

a. Department of Chemistry, University of Bari “Aldo Moro”, Via Orabona 4, 70126 Bari, Italy

b. Institute of Nanotechnology, National Research Council of Italy, c/o Department of Chemistry, University of Bari “Aldo Moro”, Via Orabona 4, 70126 Bari, Italy

c. Department of Pharmacy-Drug Sciences, University of Bari “Aldo Moro”, Via Orabona 4, 70126 Bari, Italy

### **ABSTRACT**

A novel method has been developed for the deposition of PEG containing coatings with cell repulsive properties. PEG is atomized from a water solution directly in a dielectric barrier discharge where, due to the presence of a film precursor, ethylene, a composite coating is deposited. Morphological characterization evidenced the globular appearance of the coatings due to the presence in the feed of solution droplets. The chemical characterization, and in particular the MALDI-TOF analysis confirmed the presence of PEG-like regions, in an amount decreasing with increasing the ethylene content in the film. Finally, cell culture essays highlighted the anti-adhesive characteristics of the PEG-rich deposited coatings.

### **KEYWORDS:**

Aerosol assisted plasma deposition, Atmospheric Pressure Plasma, PEG, non-fouling, surface characterization.

## **INTRODUCTION**

In the biomedical field, to prevent the non-specific interaction of cells, proteins, and microorganisms with medical device surfaces represents a crucial point in terms of device efficacy and safety [1]. To this purpose the development of materials with non-fouling properties have been the subject of extensive research within the last years [2-4]. Poly(ethylene glycol) (PEG) based surfaces are the main candidate in this topic [5-7]. The mechanism of protein resistance of PEG consists in a combination of different factors: the polymer coil forms steric repulsion preventing proteins from contacting the surface directly and then form a hydration shell around the substrate, thereby preventing the random adsorption and denaturation of proteins leading to the foreign-body reaction [8, 9]. Several approaches have been developed to modify a surface with PEG polymers, including the physical adsorption, chemisorption, grafting-from and grafting-to the surface and plasma deposition processes.

Plasma deposition processes of PEG-like coatings have been well-studied since the early 1990s [10, 11]. It allows uniform, reproducible and tuneable treatments applied to several substrates, without altering the bulk properties. Low-pressure plasma deposition processes, described in several studies published during the last two decades [12-17], showed good results concerning the synthesis/production of protein repulsion surfaces. This plasma process is based on saturated PEG-like precursors (including oligoglymes, dioxane, and crown ethers) [17]. Depending on the experimental plasma conditions, the structure of the precursor can be incorporated into the deposited coating, and the non-fouling properties of such PEG-like surfaces strongly depended on the degree of retention of glycol moiety [18]. This reason led to the use of oligoglyme precursors with more ethylene glycol units (e.g. tetra(ethylene glycol)dimethyl ether) [19]. However, due to the low vapor pressure of oligoglymes, heating is required to obtain a suitable vapour flow rate, including the gas lines and reactor walls. Atmospheric Pressure Plasma (APP) deposition is recently receiving great attention in biomedical applications to achieve comparable effects in material processing with respect to low pressure plasma [20], allowing a cheaper and easier equipment with

respect to low pressure processes. In particular, by coupling an atomizer to APP deposition process it is possible to inject in the plasma gas/vapour precursors with high boiling point or liquid solutions in form of aerosol [21-23].

In the work hereby presented, instead of plasma deposition from a suitable monomer, a novel method is proposed to produce anti-fouling surfaces: PEG containing coatings have been synthesized by using aerosol-assisted APP deposition process by spraying a PEG polymer solution directly in a Dielectric Barrier Discharge (DBD).

## **MATERIALS AND METHODS**

### **Materials**

Helium 99.999% and ethylene 99.95% (Air Liquide) were used as feed gas in the APP deposition process. Solutions (1% and 10% w/v) of PEG 35000 (flakes, Sigma-Aldrich), in water of Milli-Q quality (Millipore, Bedford, MA) were used to generate the aerosol. Shards ( $1 \times 1 \text{ cm}^2$ ) of 710  $\mu\text{m}$  thick double-faced polished crystalline silicon (100) wafers (MicroChemicals GmbH) were used as substrates for the deposition experiments. Polycarbonate films ( $1 \times 1 \text{ cm}^2$ , 0.25 mm thickness, GoodFellow) were chosen as substrate, upon washing in isopropyl alcohol, for in vitro cytocompatibility assays.

For MALDI-MS analysis, the film was peeled off and dissolved in acetonitrile: water solution (60:40, v:v). Dithranol was chose as matrix (10 mg/mL in 60% acetonitrile and 0.1% TFA), and sodium trifluoroacetate (10 mg/mL), as a cationizing agent.

### **DBD Reactor**

The homemade DBD reactor used in this research has been described in detail elsewhere, in ref [24, 25]. It consists of two parallel plates silver electrodes,  $5 \times 8 \text{ cm}^2$  wide, 3 mm apart, both covered with 0.63 mm thick alumina sheets. The power generator is connected to the upper electrode, while the lower one is ground. The electrode set up is placed in a sealed Plexiglas chamber, as wide as the

electrode assembly, such that walls can confine the gas flow in the gap. The aerosol solution was generated with a pneumatic atomizer (mod. 3076, TSI) working with He at a flow rate of 5 slm. As stated by different authors [26, 27] the diameter range of the droplets produced in similar conditions by the atomizer used in the present work is typically sub-micrometric. Ethylene was fed in the chamber at a flow rate of 5 and 10 sccm. The gas flow rate was controlled by means of electronic mass flow controllers (MSK instruments). The gas/aerosol feed was let from the shorter side of the reactor, through the plasma zone between the electrodes, and was pumped out by an aspirator located on the opposite side. Discharges were ignited for 10 minutes in continuous mode using a corona power supply (PVM500, Information Unlimited). The electrical properties of the plasma were controlled, measuring the voltage and the current delivered to the system with a high-voltage (P6015A, Tektronix) probe and a resistance type current probe, both connected to an oscilloscope (TDS 2014C, Tektronix). Experiments were carried out at input power level of  $0.8 \text{ Wcm}^{-2}$ . The applied peak-to peak voltage was kept at 5.5 kV at a frequency of 14 kHz in the experimental conditions used in this work. Before each deposition experiment, a cleaning run of the electrodes was performed by igniting for 5 min a discharge fed with a water aerosol carried by He at a flow rate of 5 slm. Substrates were positioned on the bottom electrode, always within 3 cm close to the inlet of the feed, and the chamber was purged with 5 slm He stream for 5 min.

### **Chemical and morphological characterization of the samples**

Fourier Transform Infrared Spectroscopy (FT-IR) was carried out to characterize the bulk of the coatings deposited onto silicon slices. FT-IR spectra (32 scans per analysis,  $4 \text{ cm}^{-1}$  resolution) were obtained in transmission mode with a Vertex 70V Bruker spectrometer. The spectrometer was evacuated to less than 150 Pa for 10 min before each acquisition. Spectra were elaborated by the Bruker OPUS software and normalized.

Scanning Electron Microscopy (SEM) analysis were carried out to investigate the morphology of the samples with a Zeiss Supra 40 SEM instrument equipped with a Gemini field-effect emission

gun. Analysis were carried out at an extraction voltage of 3 kV, onto samples sputter coated with a 20 nm thick Cr layer with a sputter coater Q150T by Quorum technologies.

Static Water Contact Angle (WCA) measurements were performed with a Rame´-Hart Inc, 100 goniometer (2µl drops, double distilled water).

The thickness of the coatings has been evaluated by means of an  $\alpha$ -step profilometer D120 (Tencor-Instruments), after deposition onto polished crystalline silicon and scratching part of the coating with a scalpel.

X-ray Photoelectron Spectroscopy (XPS) analysis was carried out with a PHI-5600 VersaProbe - spectrometer, using a monochromatic Al X-ray source operating at 150 W. Wide scan and high-resolution C1s, O1s, N1s, S2p spectra were acquired at 115 eV and 23.5 eV pass energy, respectively. Flood gun was used for charge compensation of the samples. The hydrocarbon component of C1s spectra was set at  $285.0 \pm 0.2$  eV as reference of the Binding Energy scale. Spectral data were processed with Multipack software.

For MALDI-MS analysis, the film was peeled off and dissolved in acetonitrile. Typically, 5 µL of the doped matrix and 5 µL of film solution were thoroughly mixed and 1 µL was applied onto the target plate. All experiments were performed using a 5800 MALDI-ToF/ToF analyzer (SCIEX, Darmstadt, Germany) equipped with a neodymium-doped yttrium lithium fluoride (Nd:YLF) laser (345 nm), in reflectron or linear positive mode, with a mass accuracy of 10 ppm or 200 ppm respectively. External calibrations were performed by using a peptide mixture provided by SCIEX. In linear MS mode, 1000 laser shots were typically accumulated by a random rastering pattern, at laser pulse rates of 400 and 1000 Hz, respectively; each shown mass spectrum was averaged on at least five single mass spectra (1000 laser shots each). The delayed extraction time was set at 450 ns. DataExplorer software 4.0 (Sciex) was used to control the acquisitions and to perform the initial elaboration of data, whereas SigmaPlot 11.0 was used to graph the final mass spectra.

## **Cell response evaluation**

PEG-composite coatings deposited onto polycarbonate substrates were tested for their cytocompatibility in terms of cell adhesion and morphology by means of Coomassie Blue staining and SEM analysis.

The immortalized endothelial cell line EA.hy 926 has been used for this study. Endothelial cells were cultured in Dulbecco Modified Eagle's Medium (DMEM, Sigma-Aldrich, Saint Louis, MO, USA) supplemented with fetal bovine serum (FBS, 10% v/v) and a 1% solution of penicillin/streptomycin. Endothelial cells were cultured at 37 °C in saturated humid 5% CO<sub>2</sub>/air atmosphere in cell culture flasks (Barloworld Scientific, UK). Cells were detached from flasks with a trypsin/EDTA solution (Sigma–Aldrich) and collected in centrifuge tubes (Falcon). Cell pellets were suspended in the medium, counted and seeded onto native and plasma-coated PC substrates (6 × 10<sup>4</sup> cells in 1 mL medium) placed in 24-multiwell plates. Cells were incubated for 3 and 48 h at 37°C, in 5% CO<sub>2</sub> air.

For Coomassie Blue staining, cells were fixed with a 4% formaldehyde/PBS solution (20 min), and stained (3 min, 0.2% Coomassie Brilliant Blue R250, 50% methanol, 10% acetic acid/) after the different culture times (3 and 48 h).

For SEM observation cells were fixed with 2.5% glutaraldehyde /0.1M sodium cacodylate solution and dehydrated using a series of alcohol/water solutions (20-100%). Finally, samples were coated with 20 nm Cr.

Cell morphology and growth on PEG-composite coatings were compared with the ones observed on CCPS (Cell Culture Polystyrene) Petri dishes.

## **RESULTS AND DISCUSSION**

### **Characterization of the coatings**

In order to try to tune the chemical composition of the coating two different PEG concentration in the aerosol solution and ethylene flow rate were tested. The morphology of PEG-composite

coatings deposited with 1% and 10% of PEG solution, and 5 and 10 sccm of ethylene, obtained by means of SEM investigation is reported in Figure 1.

From these images, it can be observed that the coatings are not flat, but they are characterized by the presence of agglomerates with different shape and size with no definite characteristics. In the case of 1% PEG solution (Fig. 1 a and b) the size of the agglomerates is smaller than the ones obtained with the 10% solution (Fig. 1 c and d). Furthermore, it can be observed that the sample deposited at higher content of PEG and lower C<sub>2</sub>H<sub>4</sub> flow rate, has much bigger agglomerates on the surface likely because of the higher content of high molecular weight PEG chains. It should be remarked that, in a previous work, it was shown that aerosol assisted plasma deposition can lead to nano-capsules containing coatings [28]. Samples investigated in this paper, however, does not display such characteristic; this confirms, as shown in the previous paper, that in order to obtain a core-shell structure with such AA-APP process the solute dispersed in the aerosol solution needs to be ionic and PEG 35000 used in this process is not an ionic compound.

Thickness evaluation by profilometer has been carried out. For PEG-composite coatings obtained with 1% PEG the thickness does not change between 5 sccm,  $490 \pm 40$  nm, and 10 sccm of ethylene,  $470 \pm 70$  nm, while for PEG-composite coatings obtained with 10 % PEG the thickness increased from  $800 \pm 70$  nm with 5 sccm of ethylene to  $1220 \pm 50$  nm with 10 sccm of ethylene.

PEG materials and PEG-composite coatings generally exhibit hydrophilic properties due to their capability of binding water molecules. In fact, as shown in Table 1, PEG-composite coatings have a substantial hydrophilic character: in particular, samples obtained with 10% of PEG exhibit lower WCA values than coatings obtained with 1% of PEG, due to the higher concentration of PEG present in the coatings. On the other hand, the wettability of PEG-composite coatings decreases when the percentage of ethylene increases, due to the hydrophobic character of polyethylene-like matrix

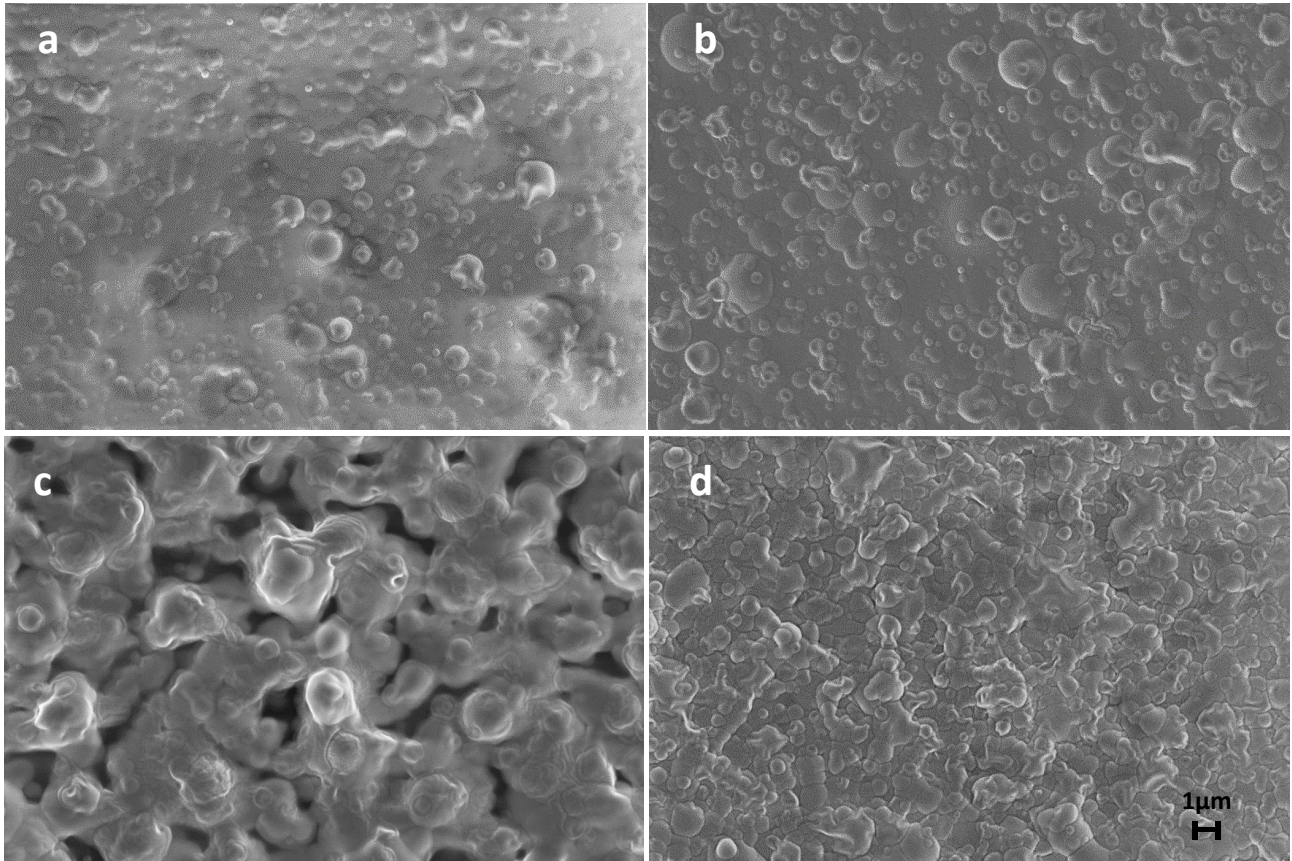


Figure 1 – SEM images of PEG-containing coatings deposited with 1%, (a and b), and 10% aerosol solution, (c and d). Ethylene flow rate of 5 sccm, (a and c), and 10 sccm, (b and d), respectively.

Table 1 – Water Contact Angle of PEG-containing coatings. Error on the values  $\pm 3^\circ$

SAMPLE	WCA ( $^\circ$ )
PEG 1%, 5 sccm $C_2H_4$	47
PEG 1%, 10 sccm $C_2H_4$	65
PEG 10%, 5 sccm $C_2H_4$	26
PEG 10%, 10 sccm $C_2H_4$	42



The FT-IR spectra of the plasma deposited coatings are reported in Figure 2 together with that of PEG 35000 drop casted sample and of a PEG-free one, plasma deposited with 10 sccm of  $C_2H_4$  and an aerosol of pure water. The spectra exhibit a common hydrocarbon backbone, revealed by the  $CH_2$  and  $CH_3$  stretching ( $2800-3000\text{ cm}^{-1}$ ) and  $CH_2$  bending ( $1480-1440\text{ cm}^{-1}$ ) absorption bands. Further, all plasma-treated samples show bands relative to  $C=O$  (stretch at  $1720\text{ cm}^{-1}$ ) and  $OH$  (stretch at  $3400\text{ cm}^{-1}$ ) testifying the oxidizing action of water fragments (O atoms, OH radicals) in the deposition mechanism [29]. The spectrum of drop casted PEG (Fig. 2A) exhibits the characteristic absorption bands of the polyethylene oxide, namely, the C-O bands at  $1050-1150\text{ cm}^{-1}$  (stretching) and at  $2800-3000\text{ cm}^{-1}$  the C-H bands, due to the stretching of  $CH_2$  and  $CH_3$  groups. The typical bands of PEG are visible in all coatings, together with those relative to the PEG-free coating.

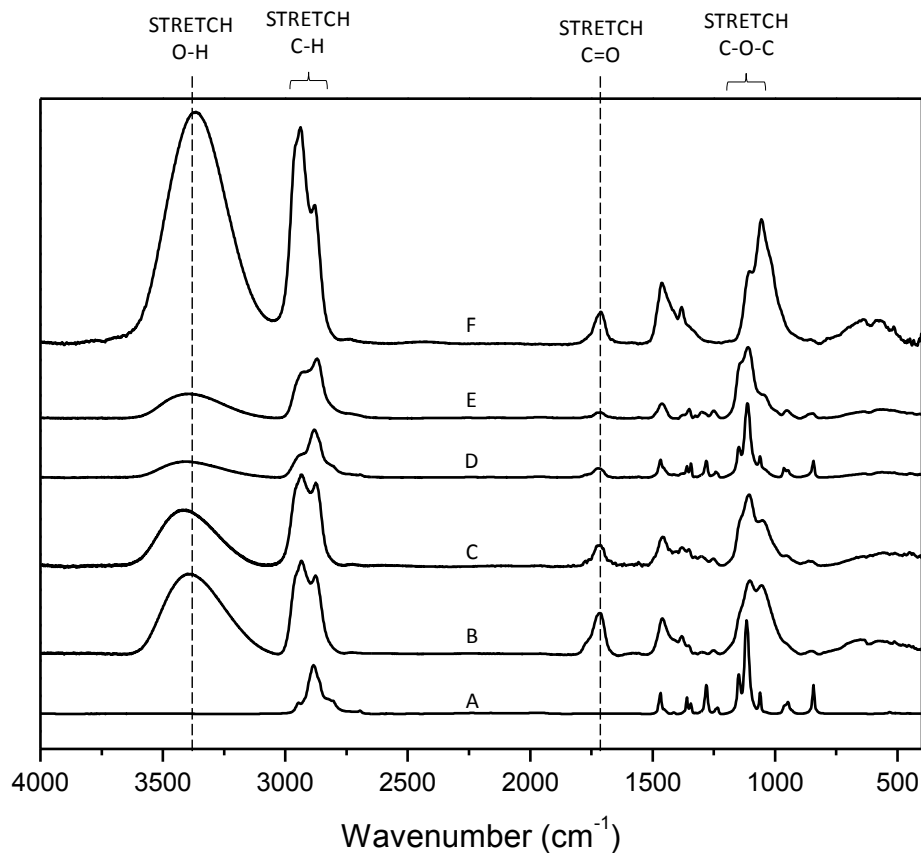


Figure 2 – Normalized FT-IR spectra of drop casted PEG 35000 (A), and coatings deposited with 1% PEG at 5 sccm  $C_2H_4$  (B) and 10 sccm  $C_2H_4$  (C), and with PEG 10% at 5 sccm  $C_2H_4$  (D), and 10 sccm  $C_2H_4$  (E), and 10 sccm  $C_2H_4$  and an aerosol of pure water (F).

sccm C<sub>2</sub>H<sub>4</sub> (E). Spectrum of a film deposited with 10 sccm of C<sub>2</sub>H<sub>4</sub> and a aerosol flow of PEG free water (F).

It is difficult to drive a correct interpretation of the bands attribution since similar bands can be found in coatings both in presence or not of PEG in the plasma. However, some observations can be drawn. As expected, the C-O region is very similar to the one of PEG when the 10% aerosol solution is used. Furthermore, it is evident that for these samples increasing the ethylene content in the feed leads to a higher importance of the bands relative to the PEG-free coating: OH stretching at 3300 cm<sup>-1</sup>, CH<sub>3</sub> stretching at 2930 cm<sup>-1</sup>, and broadening of the band at 1100 cm<sup>-1</sup>, relative to the C-O stretching.

XPS spectra show only carbon and oxygen in the deposited coatings; however, due to the addition of ethylene in the plasma phase, the chemical composition of coatings is different from that of the PEG polymer drop casted. The O/C ratio measured for PEG-composite coatings remain fairly constant around 0.26 notwithstanding the experimental conditions used, lower than the one of native PEG, 0.48. The decrease of O/C ratio is due to addition of ethylene during plasma process that increase the C content, developing the polyethylene-like matrix.

To better characterize the chemical structure of the coatings, a fitting procedure has been operated onto the C1s peak as shown in Fig. 3, and summarized in table 2: the C1s spectra were best-fitted into four peak components, each with a 1.3 eV FWHM value: C0 (285.2 ± 0.2 eV, C-H/C), C1 (286.7 ± 0.2 eV, C-OC/OH), C2 (287.9 ± 0.2 eV, C=O/O-C-O), C3 (289.0 ± 0.2 eV, COOH/COOR).

The C1s of drop casted PEG is composed not only of the C-O component at 286.5 eV, but it presents peaks at lower and higher BE, likely contaminations. In the case of the PEG containing coatings the C1s peak mostly presents an important contribution due to hydrocarbon, with a percentage in the range 61-70%, and less intense C2 and C3 peaks that only slightly change with the experimental conditions. Considering the C1 peak characteristic of the ethylene oxide unit of the PEG system, instead, it can be observed from Figure 3 and table 2, that coatings deposited with an

aerosol solution of PEG 10% have a higher content of this component, as it can be expected for the higher amount of PEG in the feed. Due to these results, it is expected that PEG-composite coatings deposited with 10% of PEG solution are less cell-adhesive than PEG-composite coatings deposited with 1% of PEG solution, due to a higher retention of glycol moieties in the coatings.

Table 2. C1s XPS best fitting summarizing table

Sample		Fitting components (%)			
		C0	C1	C2	C3
PEG Drop casted		11.6	77.8	8.3	2.3
H <sub>2</sub> O	10 sccm C <sub>2</sub> H <sub>4</sub>	82.1	14.0	3.9	//
PEG 1%	5 sccm C <sub>2</sub> H <sub>4</sub>	70.4	24.1	4.6	1.0
	10 sccm C <sub>2</sub> H <sub>4</sub>	62.9	27.6	6.9	2.6
PEG 10%	5 sccm C <sub>2</sub> H <sub>4</sub>	60.7	32.5	5.2	1.7
	10 sccm C <sub>2</sub> H <sub>4</sub>	61.9	32.4	4.8	0.8

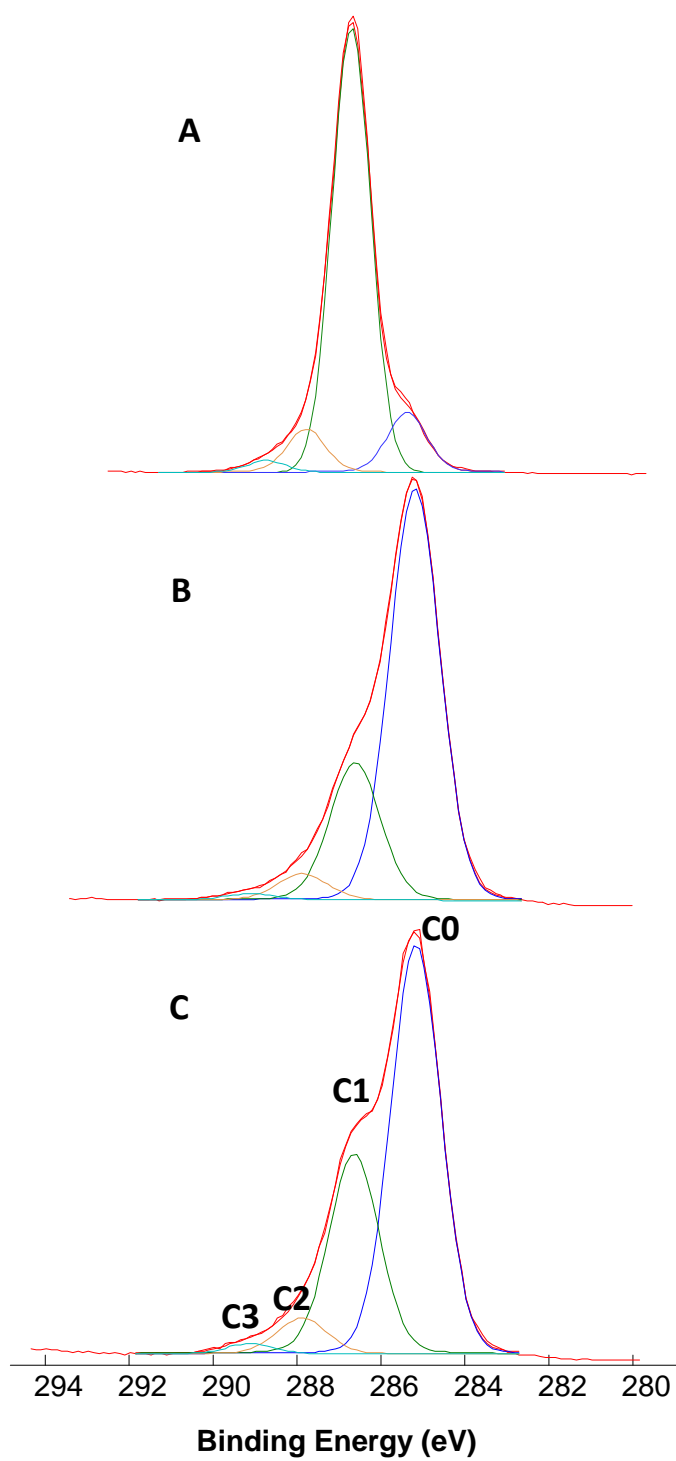


Figure 3 - C1s spectra of PEG drop casted (A), PEG containing coatings deposited at 5 sccm of ethylene with 1% (B) and 10% PEG 35000 solution (B), respectively.

To get further insights into the chemical structure of the coating, MALDI-TOF MS analysis have been performed. A standard sample of PEG 35000 was analyzed for instrumental set up and the main findings are presented and discussed in Supplementary Data. MALDI-TOF MS spectra of PEG 35000 exhibited the occurrence of two polymer dispersions, both experiencing the same monomer unit of 44.0 Da due to ethylene oxide (i.e.,  $-\text{CH}_2\text{CH}_2\text{O}-$ ) and HO- group at one end but the other end groups were respectively  $-(\text{CH}_2)_2\text{OH}$  and  $-(\text{CH}_2)_4\text{OH}$  (see Figure S1). In the case of plasma deposited PEG containing coatings, samples obtained at different ethylene flow rate and different PEG solution concentration have been analyzed. Results are reported in plots A-E of Figure 4 in which the mass spectra in the zoomed region 1200-1800  $m/z$  are displayed. It should be considered that in reflectron mode information arise mostly from soluble oligomers present in the samples; nevertheless, analytical results obtained can provide a scenario about the chemical structure of the investigated coatings. As it can be inferred from plot A, the sample deposited at the higher PEG loading (10 %) and 5 sccm of  $\text{C}_2\text{H}_4$  reveals a dispersion almost identical to standard PEG with two main polymer distributions featuring the same, above invoked, end groups. Indeed, the peaks at  $m/z$  1229.7, and the peaks series with  $m/z$  44 period (black circles in plot A), along with the corresponding distribution of peak with  $m/z$  period of 44 starting with  $m/z$  1257.8 (black squares in plot B) were detected. The number of monomers  $n$  was evaluated in both cases as described in Supplementary Data. The main difference experienced here compared to a standard sample of PEG was the greater signal intensity of peaks at low  $m/z$  range (around  $m/z$  1100), thus suggesting shortening of polymer chain under plasma treatment. Although similar results were obtained when the flow rate of ethylene in the plasma phase was increased up to 10 sccm, while the percentage of PEG remained unchanged, the distributions are of comparable intensities (plot B). The sample obtained from 1% PEG features an inversion of the signal distributions (see plot C) accompanied with the likely appearance of a different polymer. Indeed, between the ions at  $m/z$  1582.0 and 1610.0, corresponding to a number  $n$  of oligomers equal to 35 and end groups  $-(\text{CH}_2)_2\text{OH}$  and  $-(\text{CH}_2)_4\text{OH}$ , respectively, another peak signal was seen at  $m/z$  1594.0 yet not compatible with

previous assignments. Since the new distribution is again outdistanced by 44.0 Da, there is no change in the monomer unit, so the occurrence of another single end group, such as  $-(\text{CH}_2)_3\text{CH}_3$  is suggested. This is most likely related to the relative increase of ethylene in the reaction chamber. Using the peak signal at  $m/z$  1594.0, the number of monomers with HO- (17.0 Da) and  $-(\text{CH}_2)_3\text{CH}_3$  (57.1 Da) as end groups was  $n=35$  which is the same value obtained with its brother peak signals at  $m/z$  1582.0 and 1610.0. By fixing the PEG load at 1% and 10 sccm of  $\text{C}_2\text{H}_4$ , the predominant distribution was clearly evidenced (open circles in plot D) with a repetition unit of 58.0 Da between the peak signals at  $m/z$  1141.8, 1199.8, 1257.8, 1315.9, 1373.9, 1432.0, 1490.0, etc. The appearance of this additional distribution suggested the generation of another polymer featuring a propylene oxide repetitive unit (i.e.,  $-(\text{CH}_2)_3\text{O}-$ ). To validate this idea, a control sample of ethylene and water without PEG was examined (see plot E). As it can be seen, almost the same polymer distribution with repetition unit of 58.0 Da there exists, probably associated to a reaction between ethylene and water in the plasma phase. Considering the incidence of 57.0 Da of the prevailing end group (i.e.,  $-(\text{CH}_2)_3\text{CH}_3$ ) observed upon lowering the PEG content and concurrent increase of ethylene in the plasma phase, the value of  $n$  was calculated as follows:

$$n = \frac{\frac{m}{z} - 22.9898 - 17.0027 - 57.0704}{58.0419} + 1 \quad [1]$$

The experimental values of peak signals at  $m/z$  1141.8, 1199.8, 1257.8, 1315.9, 1373.9 allowed to compute the corresponding number of monomers varying from 19 to 23, respectively.

This result likely indicates that ethylene reacting with water forms a film almost independently from the presence of PEG in the feed, and in turn the deposited coating consists of PEG units embedded in an oxidized hydrocarbon matrix. On the other end it seems that at least in part the end groups of the oligomers (end likely also of the PEG longer chain) are partially modified because of interaction with the ethylene in the plasma.

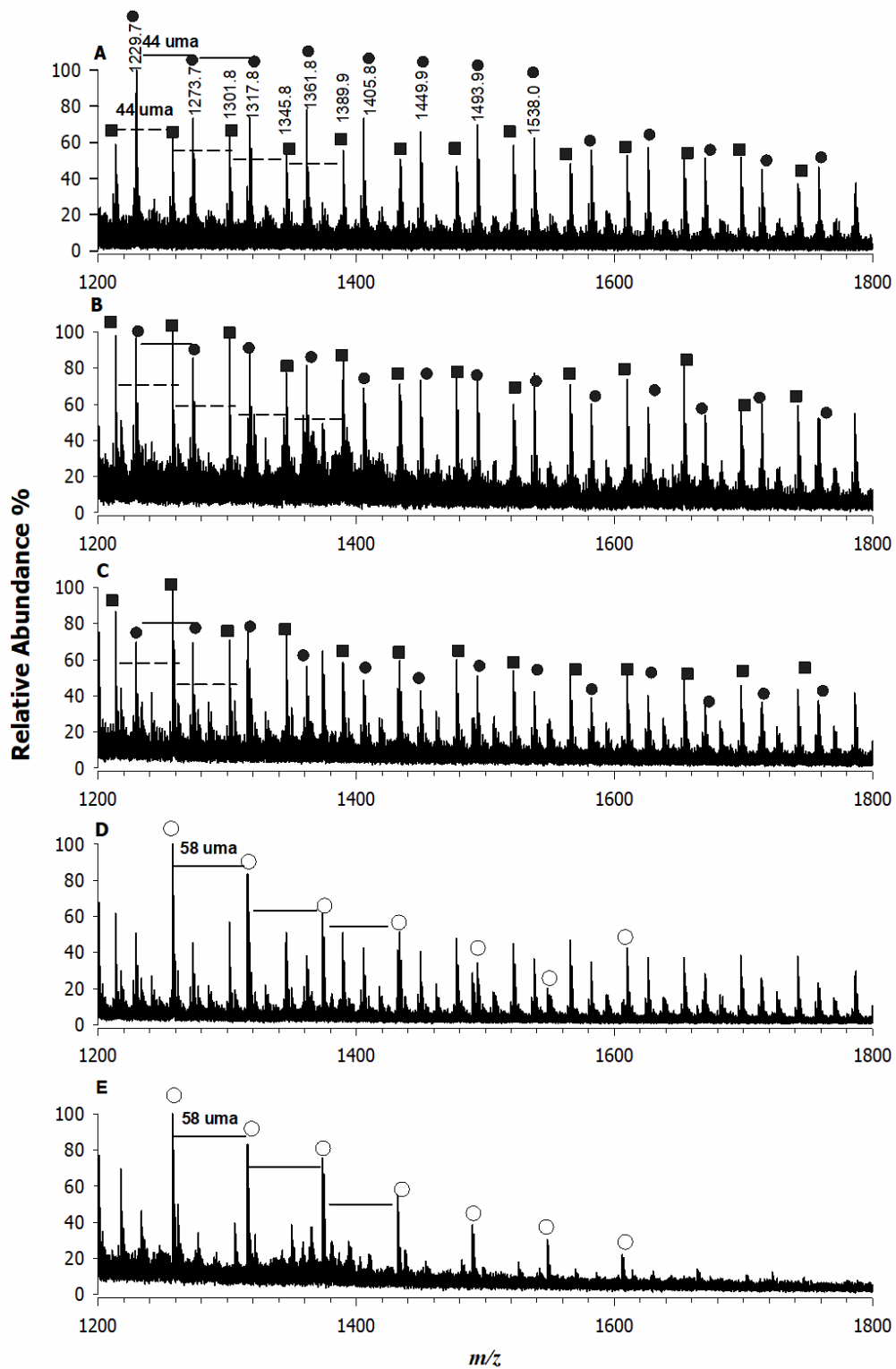


Figure 4 - MALDI-TOF mass spectra of deposited coatings with (A) PEG 10% at 5 sccm  $C_2H_4$ , (B) PEG 10% at 10 sccm  $C_2H_4$ , (C) PEG 1% at 5 sccm  $C_2H_4$ , (D) PEG 1% at 10 sccm  $C_2H_4$ , (E) a film deposited with 10 sccm of  $C_2H_4$  and an aerosol flow of water.

## Cell response evaluation

To evaluate the behaviour of cells on the different PEG-composite surfaces, endothelial cells have been seeded on PEG-composite coatings, and cell adhesion and growth were evaluated at two different times, 3 and 48 hours, by means of Coomassie Blue staining and SEM analysis. In Figure 5 a difference in cell adhesion and growth, on the different PEG-composite coatings, both at 3 and 48 hours can be easily appreciated.

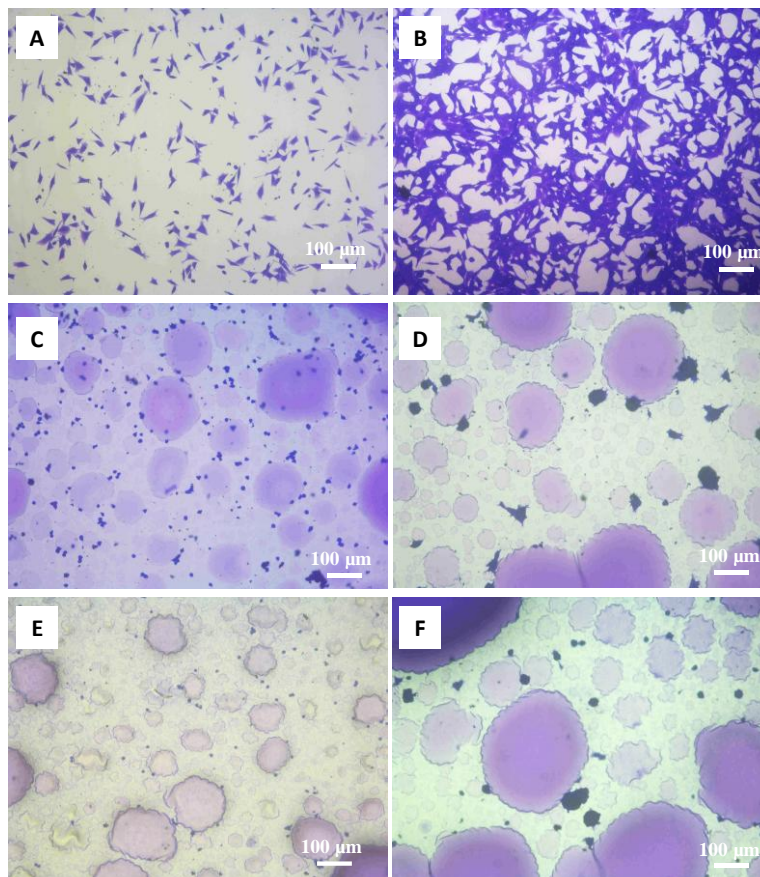


Figure 5 – Coomassie Blue staining images of endothelial cells after 3 and 48 hours, respectively left and right, on CCPS (A, B), PEG-composite coatings deposited at 10 sccm ethylene with 1% (C, D) and 10% (E, F) of PEG 35000 solution.

At a first glance, cell growth is evident only on CCPS (positive control). Proliferation of cells is present, with mostly of cells forming globular clusters after 48 hours of growth, revealing scarce



cell/material interaction as expected from non-fouling properties of PEG well known to resist protein adsorption [9].

In order to investigate the morphological aspect of cells in contact with PEG-composite surfaces, SEM analysis was performed on samples where cells were grown for 48 h. Particular attention has been devoted in examining how single and clustered cells interact with surface coatings.

A complete analysis of cells behavior, in terms of morphology, on all the different samples is evident on Figure 6 where cells clustered on different surfaces are compared, together with the picture of CCPS. As expected, very spread EA.hy 926 cells are grown on CCPS samples. Much clustered though with some elongated tails are present on PEG-composite coatings deposited with 1% PEG solution at 10 sccm. When PEG aerosol solution concentration is increased, round cells are so packed together that is very difficult to discern single cells. This analysis surely reflects the non-fouling properties of the plasma modified samples.

Passing to the analysis of single cells, as it is evident also from the Coomassie blue staining, it is hard to found single cells on CCPS, however in figure 7 corresponding SEM images for the samples deposited at 10 sccm at different PEG concentration are reported. Since spreading indicates a good affinity of cells for the substrate, in it can be observed that cells cultured on PEG-composite coatings obtained with 1% of PEG appear more spread than those grown on PEG-composite coatings obtained with 10% of PEG. In this case cells adhere with a globular morphology to minimize the membrane/material contact area, thus confirming the cell-repulsive character of the coatings.

In agreement with literature [12, 15, 17], these results confirm the relation between the chemical composition of the surface and the non-fouling property: a higher percentage of PEG in the aerosol solution, means a higher content of glycol moieties in the coating and thus a higher inhibition of cell adhesion.

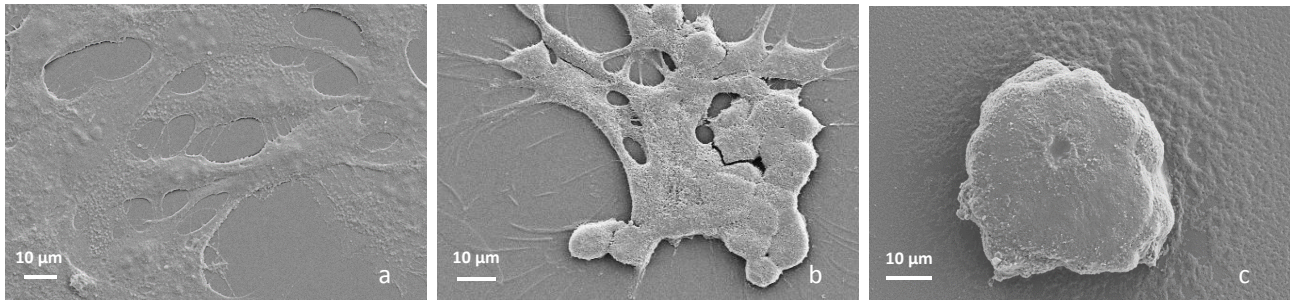


Figure 6 – SEM images of endothelial cell clusters after 48 hours on CCPS (a) and on PEG-composite coatings deposited with 1% (b) and 10% (c) of PEG 35000 solution at 10 sccm ethylene flow rate.

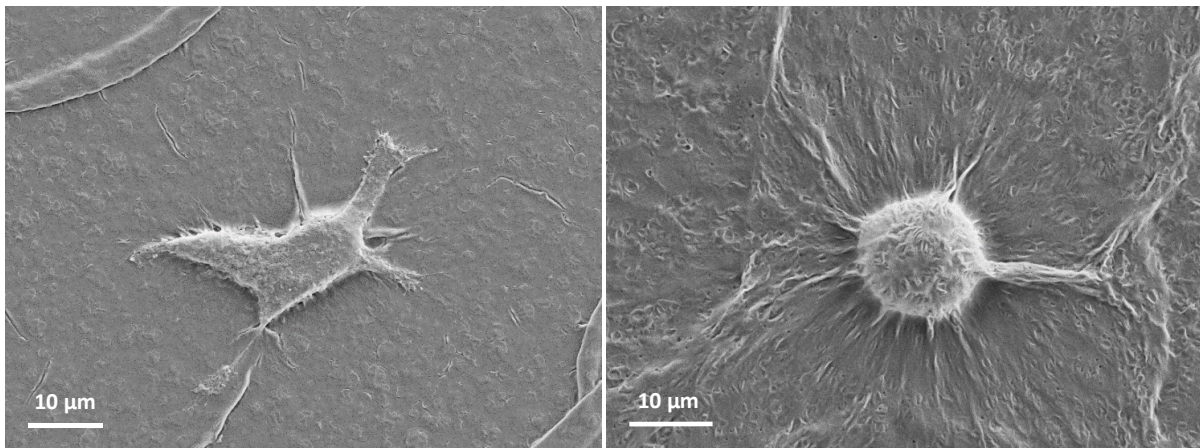


Figure 7 – SEM images of endothelial cells grown for 48 hours on PEG-composite coatings deposited with 1% (left) and 10% PEG solution (right) with 10 sccm of ethylene.

## Conclusions

An innovative method has been optimized for the deposition of PEG based coatings with non-fouling property. A PEG polymer solution is atomized in the plasma together with ethylene. The latter form a matrix entrapping the PEG domains whose presence is highlighted by mass spectra obtained by means of MALDI-TOF analysis and confirmed by complimentary XPS and FTIR. PEG content in the coating can be modulated by changing its concentration in the atomized solution and

the relative ethylene flow rate. SEM analysis show an irregular globular morphology, expected from the results obtained from analogous systems. The coatings obtained using a higher concentration of PEG in the atomizer solution (10%) exhibited a scarce endothelial cells adhesion and growth.

The method here described can be advantageously used for easy, user friendly and fast deposition of non-fouling PEG based coatings.

### **Acknowledgement**

Savino Cosmai and Danilo Benedetti are acknowledged for their skill technical assistance. The activity reported in this paper has been partly funded by Regione Puglia “Apulian Industrial Plasma Laboratory, LIPP” and the Italian Ministry for Education (MIUR) under grant PONa3\_00369 SISTEMA. A.T. gratefully acknowledges MIUR for funding her PhD course by PON FSE-FESR Research and Innovation 2014-2020.

## REFERENCES

- [1] A. Utrata-Wesolek, Antifouling surfaces in medical application. *Polimery*. **2013**, 58, 9.
- [2] H. Chen, L. Yuan, W. Song, Z. Wu, D. Li, Biocompatible polymer materials: Role of protein–surface interactions. *Progress in Polymer Science*. **2008**, 33 1059–1087.
- [3] E. Sardella, F. Palumbo, G. Camporeale, P. Favia, Non-Equilibrium Plasma Processing for the Preparation of Antibacterial Surfaces. *Materials* **2016**, 9, 515. doi:10.3390/ma9070515
- [4] M. Heuberger, T. Drobek, N.D. Spencer, Interaction Forces and Morphology of a Protein-Resistant Poly(ethylene glycol) Layer. *Biophysical Journal*. **2005**, 88, 495–504. doi: 10.1529/biophysj.104.045443
- [5] T. Tsukagoshi, Y. Kondo, N. Yoshino, Protein adsorption and stability of poly(ethylene oxide)-modified surfaces having hydrophobic layer between substrate and polymer. *Colloid Surf B*. **2007**, 54:82–7.
- [6] S.J. Sofia, E.W. Merrill, Grafting of PEO to polymer surfaces using electron beam irradiation. *J Biomed Mater Res*. **1998**, 40:153–63
- [7] Q. Chen, S. Yu, D. Zhang, W. Zhang, H. Zhang, J. Zou, Z. Mao, Y. Yuan, C. Gao, R. Liu, Impact of Antifouling PEG Layer on the Performance of Functional Peptides in Regulating Cell Behaviors. *J. Am. Chem. Soc.* **2019**, 141, 16772–16780
- [8] S.R. Meyers, M.W. Grinstaff, Biocompatible and Bioactive Surface Modifications for Prolonged In Vivo Efficacy. *Chemical Reviews*. **2012**, 112(3), 1615–1632. doi:10.1021/cr2000916
- [9] B.D. Ratner, A.S. Hoffman, Biomaterials Science: An introduction to materials in medicine. **2013** Chapter I.2.10 Non-Fouling Surfaces. pp. 241-247
- [10] G.P. Lopez, B.D. Ratner, C.D. Tidwell, C.L. Haycox, R.J. Rapoza, T.A. Horbett, Glow discharge plasma deposition of tetraethylene glycol dimethyl ether for fouling-resistant biomaterial surfaces. *J. Biomed. Mater. Res*. **1992**, 26, 415
- [11] M.N. Mar, B.D. Ratner, S.S. Yee, Grafted poly-ethylene oxide brushes as non-fouling surface coatings. *Sensors Actuators B Chem*. **1999**, 54 (1–2) 125–131
- [12] F. Palumbo, P. Favia, M. Vulpio, R. D’Agostino, RF Plasma Deposition of PEO-Like Films: Diagnostics and Process Control. *Plasmas Polym*. **2001**, 6 (3) 163–174.
- [13] R. Gristina, M. Nardulli, E. Sardella, F. Intranuovo, R.A. Salama, D. Pignatelli, B.R. Pistillo, G. Dilecce, R. D’Agostino, P. Favia Remote and Direct Plasma Processing of Cells: How to Induce a Desired Behavior. *Plasma Medicine*. **2012**, 2(1-3): 97–114
- [14] F. Brétagnol, M. Lejeune, A. Papadopoulou-Bouraoui, M. Hasiwa, H. Rauscher, G. Ceccone, P. Colpo, F. Rossi, Fouling and non-fouling surfaces produced by plasma polymerization of ethylene oxide monomer. *Acta Biomater*. **2006**, 2 (2) 165–172

- [15] E. Sardella, R. Gristina, G.S. Senesi, R. D'Agostino, P. Favia, Homogeneous and Micro-Patterned Plasma-Deposited PEO-Like Coatings for Biomedical Surfaces. *Plasma Process. Polym.* **2004**, 1 (1) 63–72.
- [16] M. Shen, M.S. Wagner, D.G. Castner, B.D. Ratner, T.A. Horbett, Multivariate Surface Analysis of Plasma-Deposited Tetraglyme for Reduction of Protein Adsorption and Monocyte Adhesion. *Langmuir.* **2003**, 19 (5) 1692–1699
- [17] E.E. Johnston, J.D. Bryers, B.D. Ratner, Plasma Deposition and Surface Characterization of oligoglyme dioxane and crown ether non fouling films. *Langmuir.* **2005**, 21 (3) 870–881
- [18] B. Nisol, G. Oldenhove, N. Preyat, D. Monteyne, M. Moser, D. Perez-Morga, F. Reniers, *Surf. Coat. Technol.* **2014**, 252, 126
- [19] B. Nisol, C. Poleunis, P. Bertrand, F. Reniers, Atmospheric plasma synthesized PEG coatings: non-fouling biomaterials showing protein and cell repulsion. *Plasma Process. Polym.* **2010**, 7, 715
- [20] E. Stoffels, Tissue Processing with Atmospheric Plasmas. *Plasma Phys.* **2007**, 47, 40.
- [21] G. Da Ponte, E. Sardella, F. Fanelli, R. d'Agostino, R. Gristina, P. Favia, Plasma Deposition of PEO-Like Coatings with Aerosol-Assisted DBD. *Plasma Process. Polym.* **2012**, 9, 1176
- [22] F. Palumbo, A. Treglia, C. Lo Porto, F. Fracassi, F. Baruzzi, G. Frache, D. El Assad, B. R. Pistillo, P. Favia, Plasma-Deposited Nanocapsules Containing Coatings for Drug Delivery Applications. *ACS Appl. Mater. Interfaces.* **2018**, 10, 35516–35525
- [23] C.P. Hsiao, C.C. Wu, Y.H. Liu, Y.W. Yang, Y.-C. Cheng, F. Palumbo, G. Camporeale, P. Favia, J.S. Wu, Aerosol-Assisted Plasma Deposition of Biocomposite Coatings: Investigation of Processing Conditions on Coating Properties. *IEEE Trans. Plasma Sci.* **2016**, 44, 3091–3098.
- [24] C. Lo Porto, F. Palumbo, G. Palazzo, P. Favia, Direct Plasma Synthesis of Nano-Capsules Loaded with Antibiotics. *Polym. Chem.* **2017**, 8, 1746–1749.
- [25] C. Lo Porto, F. Palumbo, J. Buxadera-Palomero, C. Canal, P. Jelinek, L. Zajickova, P. Favia, On the Plasma Deposition of Vancomycin-Containing Nano-Capsules for Drug-Delivery Applications. *Plasma Process. Polym.* **2018**. doi.org/10.1002/ppap.201700232
- [26] P. Heyse, M.B.J. Roeffaers, S. Paulussen, J. Hofkens, P.A. Jacobs, B.F. Sels, Protein Immobilization Using Atmospheric-Pressure Dielectric-Barrier Discharges: A Route to a Straightforward Manufacture of Bioactive Films. *Plasma Processes Polym.* **2008**, 5, 186–191.
- [27] P. Heyse, A. Van Hoeck, M.B.J. Roeffaers, J.P. Raffin, A. Steinbüchel, T. Stöveken, J. Lammertyn, P. Verboven, P.A. Jacobs, J. Hofkens, S. Paulussen, B.F. Sels, Exploration of Atmospheric Pressure Plasma Nanofilm Technology for Straightforward Bio-Active Coating Deposition: Enzymes, Plasmas and Polymers, an Elegant Synergy. *Plasma Processes Polym.* **2011**, 8, 965–974

- [28] C. Lo Porto, F. Palumbo, F. Fracassi, G. Barucca, P. Favia, On the formation of nanocapsules in aerosol assisted atmospheric- pressure plasma. *Plasma Process Polym.* **2019**; e1900116. DOI: 10.1002/ppap.201900116
- [29] Y. Yang, G. Camporeale, E. Sardella, G. Dilecce, J. Wu, F. Palumbo, P. Favia, Deposition of Hydroxyl Functionalized Films by Means of ethylene Aerosol-Assisted Atmospheric Pressure Plasma. *Plasma Process. Polym.* **2014**, 11, 1102–1111

**Declaration of interests**

The authors declare that they have no known competing financial interests or personal relationships that could have appeared to influence the work reported in this paper.

The authors declare the following financial interests/personal relationships which may be considered as potential competing interests: